Development of a front end with GNSS, 4G/5G, any other SOOP and IMU support by a customized SDR

Thomas Kraus, Mohamed Bochkati, Clovis Achy Soares Maia, Alexandru Lăpădat, *University of the Bundeswehr Munich*
Marko Cimbaljević, Ana Mitić, *NOFFZ Technologies GmbH*
Nikolas Dütsch, Thomas Pany, *University of the Bundeswehr Munich*

BIOGRAPHY

Thomas Kraus is a research associate at the University of the Bundeswehr Munich and works for the satellite navigation unit LRT 9.2 of the Institute of Space Technology and Space Applications (ISTA). His research focus is on future receiver design offering a superior detection and mitigation capability of RF interferences. He holds a master's degree in Electrical Engineering from the Technical University of Darmstadt, Germany.

Mohamed Bochkati is a research associate at the Institute of Space Technology and Space Applications (ISTA) at the University of the Bundeswehr Munich (UniBw M). His research focuses on Deeply Coupled GNSS/INS integration and novel calibration techniques for MEMS-IMUs. Before he joined the University of the Bundeswehr, he was a research associate at the Institute of Geodesy (ife) at the Leibniz University Hannover, where his research activities include quantum inertial navigation systems and GNSS receiver clock modeling. He holds a Bachelor's and Master's degree in Geodesy and Geoinformation from Technical University Munich.

Clovis Achy Soares Maia has been an Associate Professor of Physics at University of Brasilia (UnB, Brazil) since 2009 before moving back to Germany in 2022 as a Research Associate at the University of the Bundeswehr Munich. With a wide background in Physics and experience in signal detection and analysis in astrophysics, he has been working with Software Defined Receivers for GNSS signal processing and positioning under interference and jamming, as well as hybrid PNT technology with use of LEO satellite constellations.

Alexandru Lăpădat is a research associate at the Institute of Space Technology and Space Applications (ISTA) at the University of the Bundeswehr Munich (UniBw M). His research focuses on GNSS signal time synchronization for hardware delay estimation. Previously, he served as a research assistant at the Geophysical Institute (GI) of Alaska, University of Alaska Fairbanks. During this time, his research activities included the development of GNSS-based Earthquake Early Warning rupture models, waveform synthesis, and the investigation of the impact of snow on GNSS observables. He holds a Bachelor's degree in Geodesy from Technical University of Civil Engineering Bucharest and a Master's degree in Applied Earth Sciences from Delft University of Technology.

Marko Cimbaljević is an employee at NOFFZ-Forsteh Technologies. His research focus is on wireless communication systems and protocols. He holds Bachelor's degree in Telecommunication system engineering from University of Belgrade School of Electrical Engineering and Master's degree in Audio and video technologies from University of Belgrade School of Electrical Engineering.

Ana Mitić is an employee at NOFFZ-Forsteh Technologies. Her main focus is on developing algorithms for Real-Time Digital Signal Processing for various RF applications. She holds Bachelor's degree in Radio communications from University of Belgrade School of Electrical Engineering and Master's degree in Radio Engineering from National Research University Moscow Power Engineering Institute.

Nikolas Dütsch is a research associate at the Institute of Space Technology and Space Applications (ISTA) at the University of the Bundeswehr Munich (UniBw M). His main focus is on the detection and geo-location of GNSS interference sources from a LEO satellite. In 2015, he received a M.Sc Degree in Electrical Engineering from the Friedrich-Alexander-University in Erlangen-Nuremberg.

Prof. Thomas Pany is with the University of the Bundeswehr Munich (UniBw M) at the Space Systems Research Center (FZ SPACE) where he leads the satellite navigation unit LRT 9.2 of the Institute of Space Technology and Space Applications (ISTA). He teaches navigation focusing on GNSS, sensors fusion and aerospace applications. Within LRT 9.2 a good dozen of full-time researchers investigate GNSS system and signal design, GNSS transceivers and high-integrity multi-sensor navigation (inertial, LiDAR) and is also developing a modular UAV-based GNSS test bed. ISTA also develops the MuSNAT GNSS software receiver and recently focuses on smartphone positioning and GNSS/5G integration. He has a PhD from the Graz University of Technology (sub auspiciis) and worked in the GNSS industry for seven years. He authored around 200 publications including one monography and received five best presentation awards from the US Institute of Navigation. Thomas Pany also organizes the Munich Satellite

 https://doi.org/10.33012/2024.19580

Navigation Summit.

ABSTRACT

This paper outlines the development of a front end that provides four radio-frequency channels with inertial measurement unit (IMU) support. The four channels can be used for receiving GNSS, 4G/5G, or other signals of opportunity (SOOP) signals, which is within the frequency range of 10 MHz to 6 GHz. By using external mixers even higher frequency bands can be sampled, the most prominent one being the Ku-band used by Starlink downlink signals. It is based on a software-defined radio (SDR), which was customized and tuned for GNSS/INS applications for the first version. It provides precise point positoning (PPP) with an accuracy of three centimeters. Therefore, a correction of the absolute frequency needs to be applied, which value depends on the selected frequency band. The IMUs are directly connected to the SDR, which are synchronized to the radio-frequency data. The synchronization is realized with the FPGA and an external IMU interface. Additionally, an automatic gain control (AGC) and a decimation of the bit resolution to reduce the data throughput is implemented within the FPGA, which allows to use the maximum analog bandwidth of 80 MHz per channel and enhances the stability of the front end. The source code of the host and FPGA is available to enable the adaption to future research work with new signals for navigation purposes.

I. INTRODUCTION

The Institute of Space Technology and Applications of the University of the Bundeswehr Munich together with NOFFZ GmbH developed a four channel front end with inertial measurement unit (IMU) support. The four channels can be used for receiving GNSS, 4G/5G, or other signals of opportunity (SOOP) signals for further digital signal processing (DSP). A maximum RF frequency of 6 GHz is possible as well as a sampling rate of 100 MHz with an analog bandwidth of 80 MHz. The bit-width ranges from 2-bit to 16-bit and numerous options for analog and digital gain control can be configured. Two type of IMUs (Micro-electro-mechanical systems (MEMS) Xsens, tactical-grade iFOG) are supported to enable the realization of an inertial navigation system (INS) development. RF signal samples and IMU data are synchronized at FPGA level with utmost accuracy and stability of microseconds. Currently, the firmware allows storing data on the hard drive of a connected PC but later developments will target real-time streaming. The front end is based on the Universal Software Radio Peripheral (USRP), which is customized with the support of the company NOFFZ Technologies GmbH. This new front end represents the baseline of future research work with our in-house software receiver, Multi-Sensor Navigation Analysis Tool (MuSNAT) (Pany et al., 2019; Arizabaleta et al., 2021). The idea is to share our front-end development with other academic non-profit research activities on request. This paper describes the architecture of this front end and provides performance values for high-precision positioning for both GNSS standalone and with INS, where three centimeter accuracy has been achieved. In the first version, the front-end software is provided with a pure record function for post processing. Later, the connection to any software receiver is realized as generic real-time front-end interface via TCP/IP, which has been once described in (Pany et al., 2019).

The USRP-2955 of NI was selected as the SDR because it offers four separate radio-frequency (RF) channels, which are provided with a very high signal quality due to the superheterodyne receivers. In addition, all frequencies can be set independently over a wide frequency range, which is especially essential for positioning solutions with 4G, 5G, or SOOP. The USRP has a general-purpose input/output (GPIO) connector, which is used for the data transfer and the synchronisation of the IMUs. The USRP-2955 is identical in construction to the model X301 with the RF daugtherboard TwinRX from Ettus Research LLC, but the USRP-2955 uses the ecosystem of NI with LabVIEW as programming tool. This allows an easy modification of the field-programmable gate array (FPGA) of the USRP. We need the FPGA modification for two reasons: a) the data reduction of the data streams by a selectable bit decimation in conjunction with an automatic gain control (AGC) and b) the data transfer and the synchronization of the IMUs via the GPIO interface. The reduction of the data size brings a higher stability for the real-time processing and the synchronization of the IMU with the RF data stream is mandatory for a successful fusion of both GNSS and IMU signals on different levels, e.g. loose coupling (LC), tight coupling (TC) and ultra-tight coupling (UTC) GNSS/INS. The supported IMUs are a commercial MEMS IMU (Xsens MTi-G-710) from Movella Inc. and a tactical grade FOG IMU (iFOG-IMU-1-A) from the iMAR Navigation GmbH. The performance of the high-precision GNSS standalone solution and the fused GNSS/INS solution will be provided in a separated section.

A final discussion deals with the frequency accuracy and precision of the USRP-2955. We observed a difference between selected and achieved frequency for some GNSS frequency bands of approximately 0.75 Hertz. The largest offset can be observed at the E5a frequency, which is visible through a large drift in the code-minus-carrier (CMC) measurement. The main driver of the offset might result from the fractional-N mode operation of the two frequency synthesizers within each RF channel. Unfortunately, the USRP-2955 does not support the integer-N mode even though it is natively available in the built-in frequency synthesizers from Analog Devices. The ecosystem of Ettus Research does support the integer-N mode and a comparison will be provided. The value for the correction of the frequency offset, which is essential for high-precision navigation, is empirically evaluated. With this adaption, we've achieved an excellent performance in RTK and PPP. Future work tries to operate the integer-N mode with the USRP-2955, even that it is not directly supported by NI at the time of writing this paper.

II. ARCHITECTURE OF THE FRONT END

Our front-end development for the software receiver (MuSNAT) is based on the USRP-2955. The programming is done in the ecosystem of NI with LabVIEW. It can acquire four RF signals in the frequency range of 10 Hz and 6 GHz with a maximum bandwidth of 80 MHz. A customized solution by us can acquire additionally two IMUs synchronized to the RF signals. A PC is connected to the USRP and records the data to a hard drive for post processing. Later developments allows a direct connection to an application for real-time processing, e.g. to our software receiver (MuSNAT). Therefore, our front end is called MuSNAT front end (MuSNAT-FE) within this paper. The described architecture is sketched in Figure 1 and a picture of the front end with the connected IMUs is given in Figure 2.

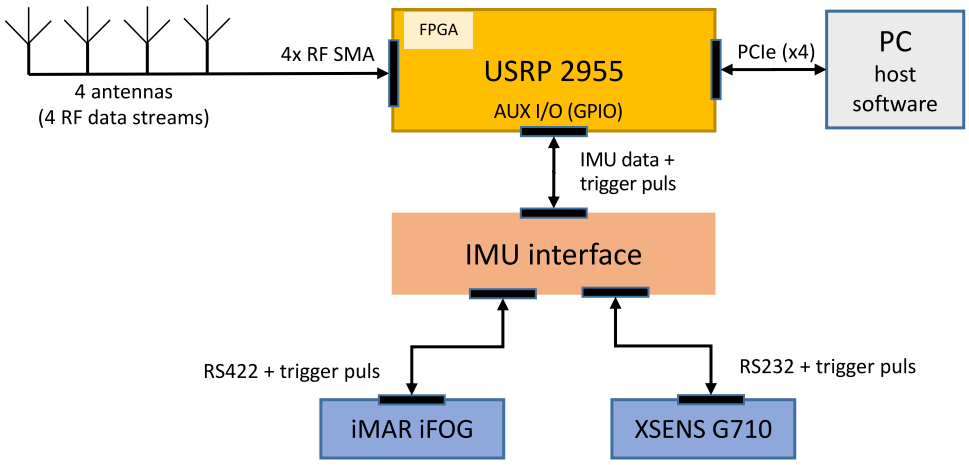

Figure 1: Architecture of the MuSNAT front end (MuSNAT-FE)

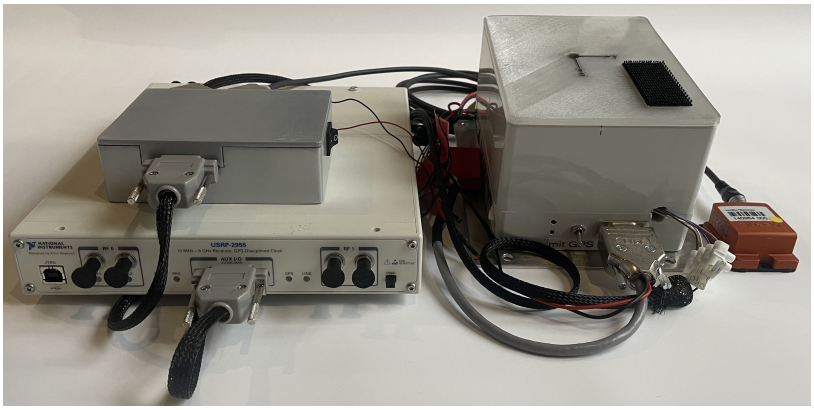

Figure 2: MuSNAT-FE with two IMUs (from left to right): USRP-2955 and PCB board to connect the iFOG (grey box) and the Xsens (orange box)

The starting point for our software development is the template of NI with "NI-USRP Simple Streaming with USRP-2945/2955". It includes the host code for the PC and the FPGA code, which runs entirely with the LabVIEW programming environment. The features of the example code can be summaries as following:

- Recording of up to four RF channels
- Simultaneous recording of four channels with a maximum bandwidth of 50 MHz (the quantization is fixed to 16 bit and the maximum data throughput from the USRP to the PC is 800 MByte/sec)
- FPGA source code in LabVIEW for the framework functions (e.g. PCIe communication, USRP configuration, ADC data acquisition, DSP processing, data transfer to the host via PXIe)
- GUI (see Figure 3) and source code for the host system
- Allows recording of an antenna array (because of three local oscillator sharing options: independent, companion, and exported & shared)

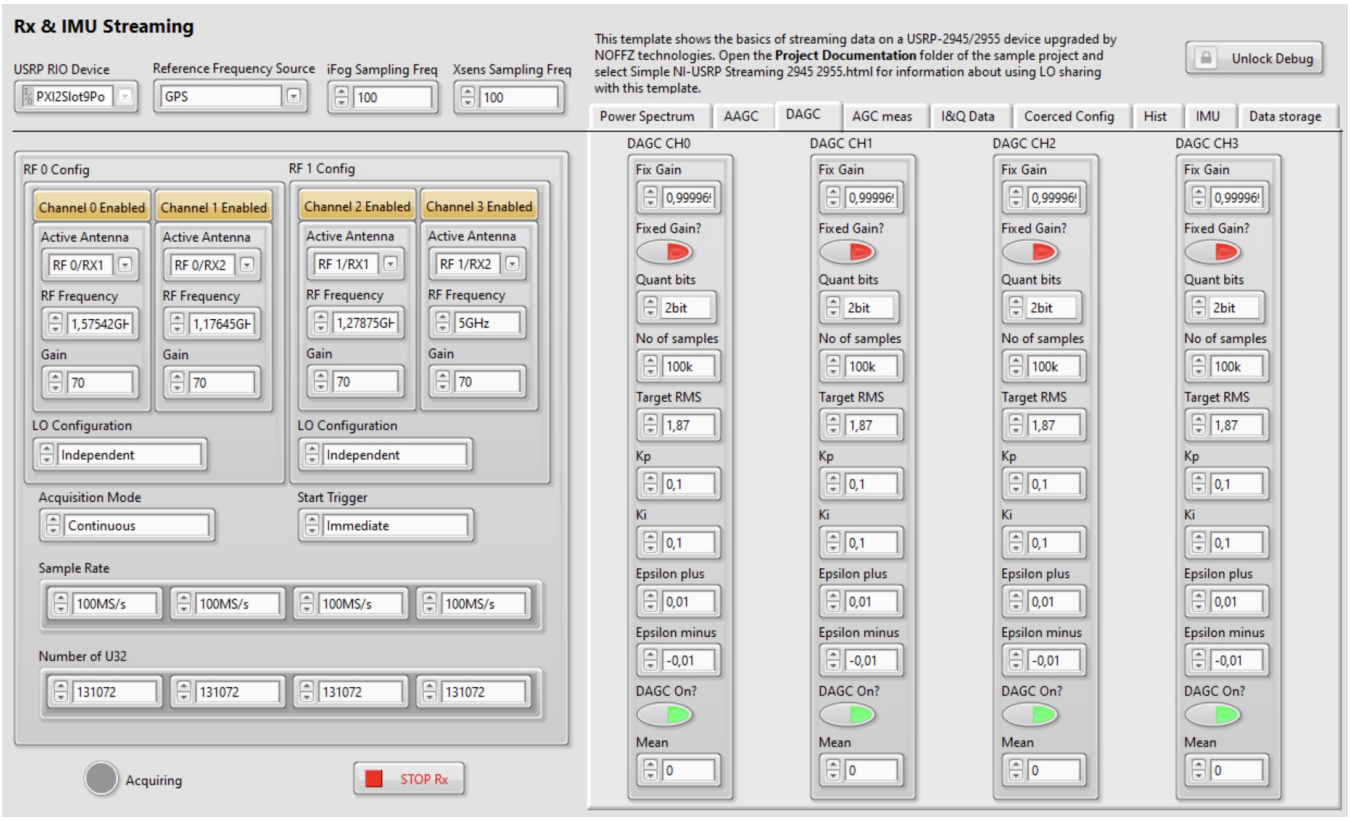

Figure 3: GUI of the MuSNAT-FE (based on a example file of NI LabVIEW)

The software is modified to enhance features of the USRP to get a front end for an high-precision navigation system with IMU support. Therefore, the IMUs are connected over the GPIO interface of the USRP to acquire the IMU data and to guarantee a synchronization with the RF data. The IMU interface establishes a physical connection between the USRP and the IMUs. For this purpose, a PCB board was designed with a 15-pin connector to the GPIO interface of the USRP and two 9-pin connectors for the UART interfaces to the IMUs: one connector for the iFOG and the other one for the XSense. The IMU interace includes integrated circuits for the adaption of the digital signal levels between the GPIO and the UARTs. The synchronization of the IMUs and reception of the IMU data directly occurs on the FPGA level. In order to achieve higher bandwidths for the RF channels, the quantization is decimated from 16 bits to either 8, 4 or 2 bits within the FPGA. This measure also contributes to greater stability, as the USRP does not have to be operated at its performance limit. Due to the reduction in the quantization, the implementation of an AGC becomes mandatory. The MuSNAT-FE enables the MuSNAT receiver to get to a high-precision navigation system with GNSS and IMU support. In case of GNSS with even three frequency bands, it allows to add further signals of opportunity such as LTE, 5G, Starlink or future signals for PNT solutions with a potential LEO orbit extensions. The added features of the MuSNAT-FE by our customization can be listed as:

- Tuning the accuracy of the selected center frequencies for various frequency bands to guarantee high-precision navigation by GNSS.
- Recording and storage of the synchronized RF and IMU data on host system
- Generation of trigger pulses for the IMUs within the FPGA at a selectable clock rate and output of these pulses for the IMUs via GPIO interface of the USRP (also named AUX I/O)
- Bit decimation of the digitized input data stream to 2, 4, and 8 bits directly on a the FPGA. The native 16-bit recording is still selectable.
- Automatic gain control (AGC) for the gain of the USRP and the digital gain by DSP for the bit decimation.
- Adjustable USRP data recording bandwidth from 10 MHz, 20 MHz, 50 MHz and 100 MHz. The maximum analog bandwidth is fixed to 80 MHz.
- Complete configuration of all parameters through GUI (e.g. USRP settings, AGC, IMU configuration, bit decimation)

During the evaluation of the MuSNAT-RF, we have realized that the accuracy of the selected frequency of the USRP is not

as expected. Unfortunately, this accuracy is dependent to the various frequencies and there is no high-precision PVT possible without knowing of these differences. This topic is discussed later of how to avoid this errors in accuracy of the frequency or how to compensate it for a precise point positioning solution.

III. IMPLEMENTATION OF THE AUTOMATIC GAIN CONTROL

The USRP-2955 has originally no AGC implemented, because the data from the 14-bit ADC are transferred in a 16-bit format from the USRP to host. This implementation limits the maximum bandwidth to 50 MHz with a simultaneous transmission of four channels. In order to achieve the USRP's maximum analog bandwidth of 80 MHz, we have to reduce the quantization of the amplitude. Therefore, a re-quantization needs to be applied to get a lower resolution of the amplitude. It is common to use a two-bit resolution for GNSS as the signal loss is only less than 0.6 decibel at an optimum signal level (Lotz, 2008). Additionally, the reduction of the data by re-quantization leads to a more stable front-end implementation and the amount of data to store on a hard drive are significantly reduced.

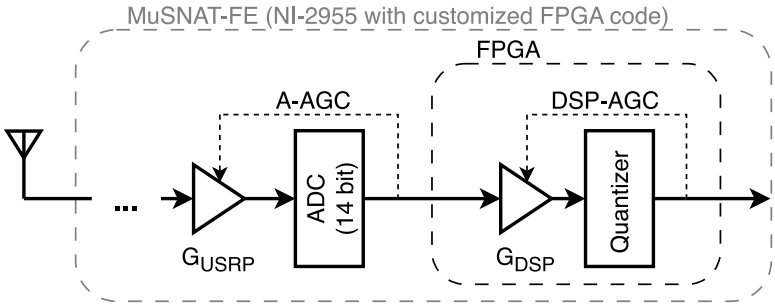

Figure 4: Implementation of the AGC for the MuSNAT-FE

For the MuSNAT-FE, we applied a two step AGC implementation, which is visualized in Figure 4. One controls the analog gain of the USRP, G_{USRP}, and the second one applies a gain control by DSP, G_{DSP}, on the FPGA. The analog AGC (A-AGC) has the task to provides a high signal quality and to avoid any saturation. The AGC by DSP (DSP-AGC) applies the conventional AGC for GNSS. There is an option implemented which stops the A-AGC after successful steering within a given time frame. The DSP-AGC is realized by a proportional-integral controller (Lotz, 2008) to achieve with a uniform and non-centered quantization a Root Mean Square (RMS) power of 1.867 for a two-bit resolution (this RMS power minimizes the quantization losses). The A-AGC is implemented as proportional controller and steers the power within a lower and upper threshold level.

The reason to use this two step AGC implementations had to reasons. First of all, the gain of the USRP-2955 is controlled by two programmable attenuators and it provides a gain from 0 dB up to 90 dB with a 0.5 dB step size. More details about the RF signal chain for GNSS signals can be found in (Arizabaleta et al., 2021). The programmable attenuators could imply a variation of the group delay, which we wanted to avoid even that they are just small. The second reason is that we prepare the front end for real-time mitigation of radio-frequency interference (RFI) directly with the FPGA. The instantaneous dynamic range of a 14-bit ADC is large enough to handle RFI and GNSS signals at the same time. The pre-correlation mitigation would be implemented just before of the DSP-AGC.

IV. IMPLEMENTATION OF THE IMU INTERFACE

The MuSNAT-FE has the option to connect two IMUs at the same time, which are internally synchronized to the radio-frequency data. They are connected to a IMU interface, which is plugged to the AUX I/0 (GPIO) connector of the USRP (see Figure 1). The IMU interface is designed and manufactured by NOFFZ technologies and the PCB layout is provided to our institute. The main task of the interface is to adapt the different digital signal levels of the USRP and the IMUs. The USRP-2955 uses transistor-transistor logic (TTL) with 3.3 volt and the IMUs have two RS-422 lines for the iMAR iFOG and two RS-232 lines for XSENSE MTI-G-710. Each IMU has two UART lines, where one is for the data transfer and the other for the synchronization. The time-critical requirements are implemented in the FPGA, which can be divided into the following four tasks:

1. **Clock loops** – Produce trigger signals for the synchronization of the IMUs on respective AUX I/O pins of the USRP-2955. The trigger signal is a square wave with the uneven duty cycle, which is necessary for iMAR-iFOG-1-A-SP-UI data timing. By modifying controls in the host application, it is possible to change the frequency of the trigger signal. It is adjustable in the range between 100 and 400 Hz, as it is required.
2. **Read data loop XSENS** – It is based on the state machine with two states: *Idle* and *ReadData*. The state machine stays in the *Idle* state until the user starts the acquisition from the host application, which will cause a change of the state to *ReadData*. The loop rate is adjusted to fit the configured baud rate of the XSENS MTi-G-710 so that every bit could be interpreted as it is. Acquired bits are transferred to the *Assembling data loop XSENS* using the target scoped FIFO of the

FPGA.

3. **Assembling data loop XSENS** – It is based on the state machine with four states: *Idle, WaitFallingEdge, Select Byte* and *Decode*. Owning to the configured baud rate, every delivered packed from the XSENS MTi-G-710 is preceded with the sequence of zero bits so it is easy to distinguish the packet from the rest of the signal. In the *Select Byte* state, the packet is assembled (stop and start bits of every byte are removed and the packet is prepared for transferring to the host application). The transfer of the packet to the host application is performed in the *Decode* state via *DMA Target to Host FIFO*.
4. **Read data loop iFOG** – It is based on state machine with three states: *Idle, Wait Falling Edge* and *Get Packet*. The state machine stays in the *Idle* state until the user starts the acquisition from the host application, which will cause a change of the state to *Wait Falling Edge*. In the *Get Packet* state, the loop is receiving bits from the respective AUX I/O pins. Similarly to *Read data loop XSENS*, this loop is adapted to fit the baud rate of the iIMAR iFOG IMU as well, so that every bit could be interpreted as it is. The size of the iFOG packet is fixed, due to its non-adjustable configuration. This fact is used when transferring and assembling its data.

V. GNSS SOFTWARE RECEIVER AND INS SOFTWARE

The detailed post-processing evaluation tool chain employed in this work is depicted in Figure 5. In the first stage, the relative time stamp of both IMUs generated by the USRP trigger puls, i.e. starting by zero, has to be converted to a superior GPS time stamp. For this reason, we processed the collected IF-samples collected during the measurement camping and processed them by means of our in-house SDR MuSNAT. After decoding the navigation message, the expected GPS-time stamp of the first

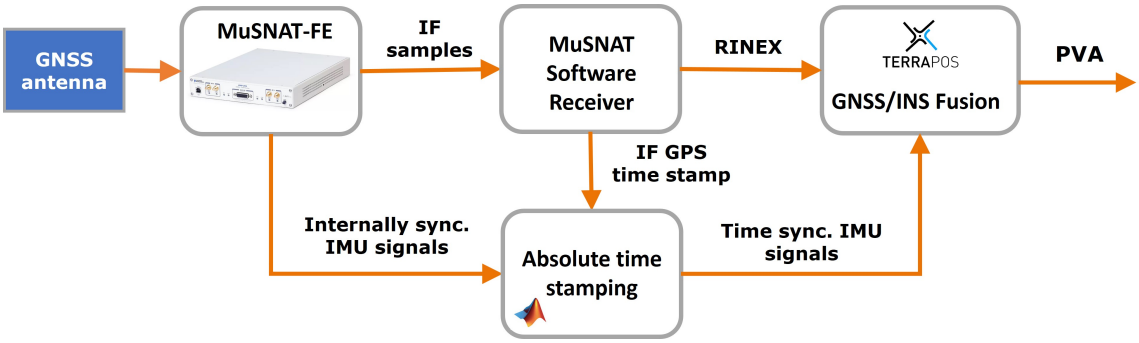

Figure 5: Post-processing evaluation tool chain

computed IF-sample can be retrieved. Thus, using this important information, the relative time vector of both connect IMUs can be attached to GPS time scale. This task, has been performed externally with a self-developed MATLAB-routine. In the final stage, using the commercial Terratec's GNSS/INS TerraPOS-software, *version 2.5.9p1* (Kjørsvik and Brøste, 2009), the generated Receiver Independent Exchange Format (RINEX) observation files produced by MuSNAT (Pany et al., 2019) as well as the time synchronized IMU signals have been processed in different coupling modes, i.e. GNSS-only, Loosely Coupled (LC) and Tightly Coupled (TC). Finally. the resulted Position Velocity and Attitude (PVA) information can be used to asses the performance of the entire navigation tool chain.

VI. EVALUATION OF THE FRONT END (PERFORMANCE)

1. Experimental Setup

In order to evaluate both performance and accuracy of the front-end hardware/software realisation, a measurement campaign under open sky conditions has been conducted. As depicted in Figure 6, the customised MuSNAT front end (2) was connected via a signal splitter to the Trimble Zephyr 2 geodetic antenna (1) to record IF-samples at 20 MHz. For validation reasons, as it will be described in Section VII, a second USRP(-X310) (5) run by the the open-source GNU Radio companion (GNU Radio project, 2022) was also connected additionally to the main antenna on top of the measurement vehicle, while sharing a common Oven-controlled Crystal Oscillator (OCXO) clock (6) with the main front end, i.e. MuSNAT-FE. IMU data (accelerations and rotation rates) from both MEMS Xsens MTI-G-710 (3) and the tactical grade FOG IMU (iFOG-IMU-1-A) IMU (4) were also collected at a sampling rate of 200 Hz and 100 Hz, respectively. The collected signals from both IMUs and front ends are stored on a data logging PC for later analysis and post-processing purposes. Furthermore, as reference GNSS receiver, the Trimble NetR9 (8) was also connected to the same antenna realising a zero-baseline configuration with the front end. To enable RTK carrier-phase positioning, a reference station with a Trimble NetR9 (is not shown in this picture) was running on top of the highest building of the campus during the measurement campaign. The trajectory contains both static and dynamic scenarios. The first scenario, the data were acquired for around 4 minutes, afterwords a dynamic dive in eight-turns at approx. 30 km/h took place. An overview about the surrounding conditions during the conducted measurement campaign can be seen in Figure 7.

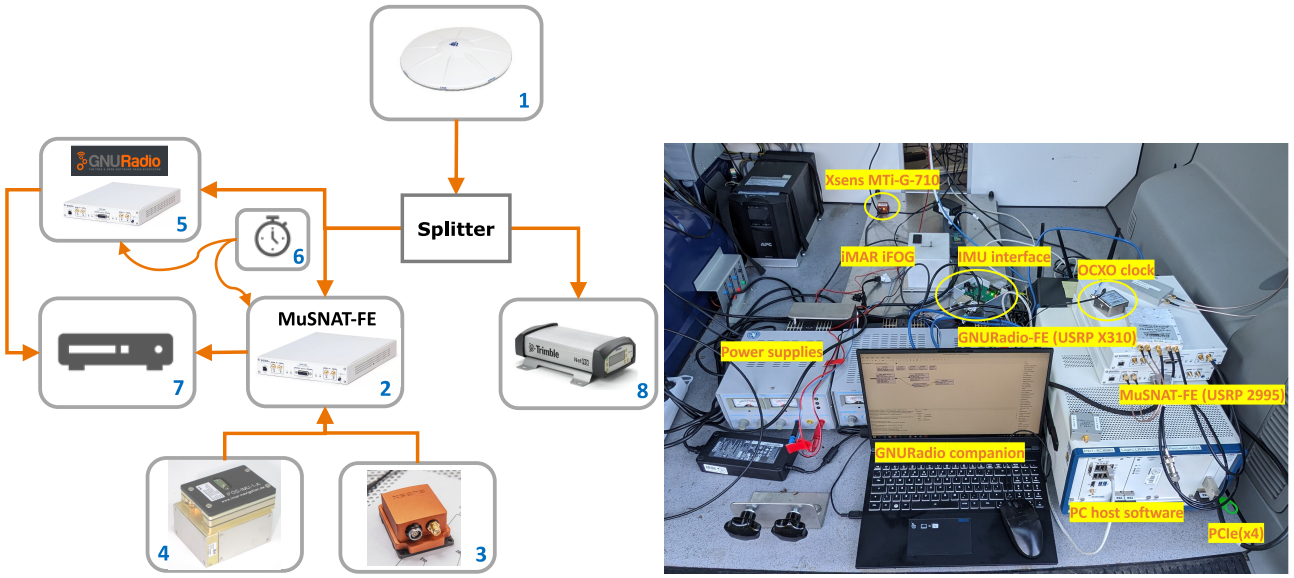

Figure 6: Hardware setup employed for the car experiment. Right picture shows the set-up as it was mounted in the back of the test vehicle, the reference Trimble GNSS receiver was mounted in the front sets, thus not possible to see it here.

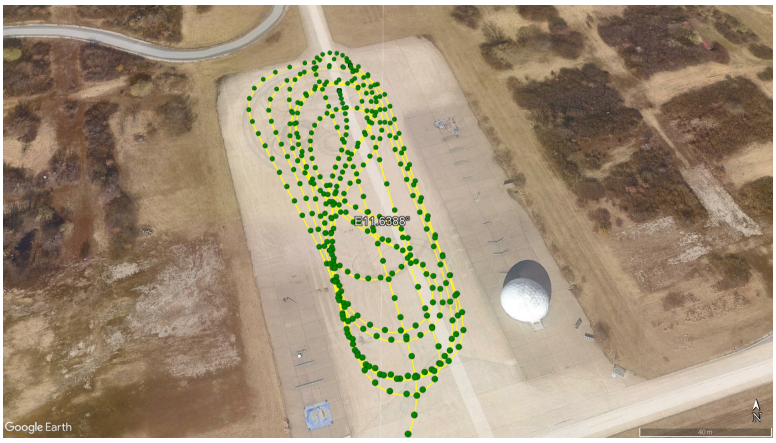

Figure 7: Trajectory overview with open-sky conditions conducted at the UniBw M test track in Neubiberg, Germany

2. Analysis

To analyse the outcome of the conducted measurement campaign, the following key performance parameters will be used in this part to highlight different aspects of the collected satellite and IMU data, including their drawback. The first parameter would be the so-called Code-minus-carrier (CMC), which is standard routine to check for gross cycle-slips or code multipath, which in turn indicates if the tracking, e.g., Phase Locked Loop (PLL), is working properly. In addition, the deviation of the computed trajectory (GNSS-only and the loose-coupled version with the different IMUs) w.r.t., to the ground-truth, which is build from the TC solution (Titterton and Weston, 2005) of the reference NetR9-receiver and the iFOG-IMU, will be shown. The achieved accuracy will be also used for this analysis. An other parameter which should be considered, is the accuracy and precision of the computed GPS time stamp for the IMU device. Fortunately, the employed TerraPos-Software offers a sophisticated option to estimate the IMU timing bias based on a Extended Kalman Filter (EKF) implementation.

For better understanding of the analysis results we may define following abbreviations:

- $\Delta P_{\text{MuSNAT-FE}}$ = the deviation of the GNSS-only positioning solution computed from the RINEX observation obtained by the MuSNAT-FE w.r.t. the reference trajectory, i.e. TC-GNSS (Trimble NetR9)/INS(iFOG)
- ΔP-LC$_{\text{MuSNAT-FE + iFOG}}$ = the deviation of the LC positioning solution computed from the RINEX observation obtained by the MuSNAT-FE and the iFOG-IMU raw signals w.r.t. the reference trajectory.
- ΔP-LC$_{\text{MuSNAT-FE + Xsens}}$ = the deviation of the LC positioning solution computed from the RINEX observation obtained by

the MuSNAT-FE and the Xsens-IMU raw signals w.r.t. the reference trajectory.

- $\Delta P_{GNURadio}$ = the deviation of the GNSS-only positioning solution computed from the RINEX observation obtained by the GNU Radio frontend w.r.t. the reference trajectory.
- σ in Figure 9 and Figure 10 (right sub-plot) refer to the computed standard deviation of the absolute trajectory as estimated by the processing software, i.e. TerraPos.
- Similarly, for the velocity deviation, only the letter "V" have been introduced after the Δ

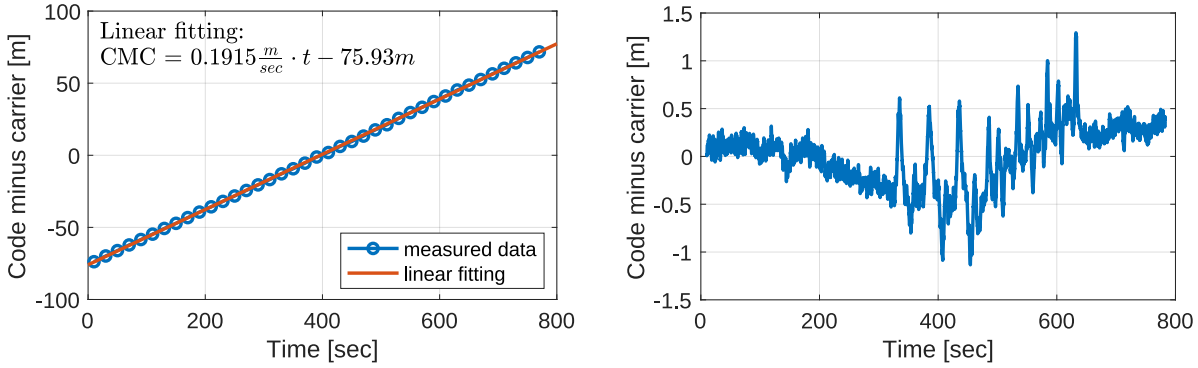

(a) **(b)**

Figure 8: Code-minus-carrier (CMC) for GPS L5: (a) a drift occurs without a calibration of the frequency offset and (b) no drift is visible when a frequency offset of 0.75 Hertz is applied

Figure 8 provides two plots of the code-minus-carrier of a GPS L5 signal. The first one shows a large drift of the CMC of 0.1915 meter per seconds. This drift is not acceptable to obtain a PPP solution. The drift of the CMC is caused by a systematic inaccuracy in the frequency by the USRP. Our investigations revealed that this error is dependent on the frequency band. There is a negligible error for the frequency bands E1/L1 and E6. However, a correction of 0.75 Hertz is required for E5a/L5 and L2 in order to obtain an approximately constant CMC. Figure 8(b) demonstrates the effect of the correction on the CMC curve for a GPS L5 signal. This value for the frequency offset has been determined empirically and it is only a temporary solution with an acceptable inaccuracy, which allows PPP with an accuracy of three centimeters. The reason for this frequency offset comes from the PLL synthesizer of the USRP, which operates in the so-called "fractional mode". This topic is discussed in detail in Section VII.

The frequency offset to the carrier frequency, Δf_c, was determined by a linear curve fitting of the CMC from Figure 8(a). The fitting provides the following result

$$\text{CMC} = \partial\text{CMC} \cdot t + \text{CMC}_{initial} \tag{1}$$

$$\text{CMC} = 0.1915 \ \tfrac{m}{sec} \cdot t + 75.93 \ m, \tag{2}$$

with a drift of the CMC for L5, $\partial\text{CMC}_{\text{L5}}$, of 0.1915 meter per seconds. This estimated drift can be used to obtain the offset of the frequency to the carrier frequency by the following equation

$$\Delta f_c = \partial\text{CMC} \cdot \frac{f_c}{c} \tag{3}$$

$$\Delta f_{c,\text{L5}} = 0.1915 \ \tfrac{m}{sec} \cdot \frac{1176.45 \text{ MHz}}{c} \approx 0.75 \text{ Hz}, \tag{4}$$

which results in an frequency offset of 0.75 Hertz. We also tested a second USRP-2955 and it demonstrated that such frequency offsets have always the same values.

As stated in the previous paragraph, Figure 9 and Figure 10 (left sub-figures) depict the deviation of the positioning results w.r.t. the reference trajectory, expressed in East-North-Up (ENU) local-frame. There it can be seen, at the first glance, that the GNURadio-FE trajectory exhibits the lowest position deviation with a Root Mean Square (RMS) smaller than 5 mm in all three components. The maximum visible difference can be observed in the north direction which is 1 cm (see Table 1). On the other hand, the MuSNAT-FE GNSS-only positioning solution, i.e. $\Delta P_{\text{MuSNAT-FE}}$, shows a degraded accuracy, albeit on the RTK-accuracy-level, i.e., $\pm$1-2 cm. Here, the highest RMS-values belongs to the up-component (1.8 cm). Furthermore, all carrier-phase ambiguities have been fixed to 100%, successfully. It has also to be mentioned, that the standard deviation of the

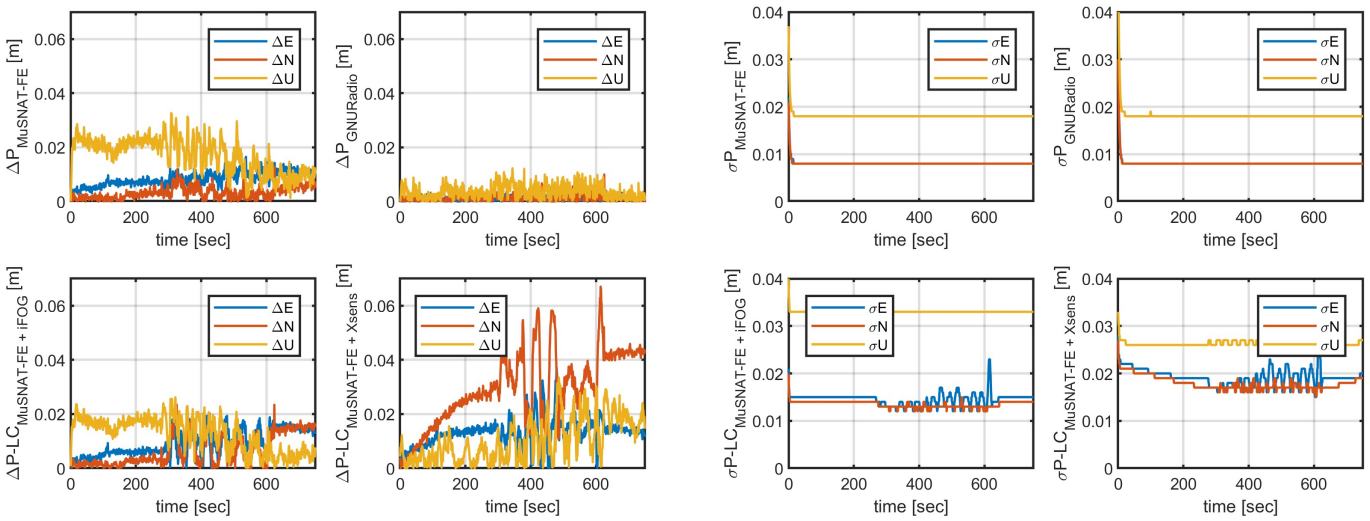

Figure 9: Deviation of the estimated position w.r.t. the ground-truth trajectory (left sub-plots) in east, north and upward direction. Right figures show the position standard deviation as estimated by TerrPos.

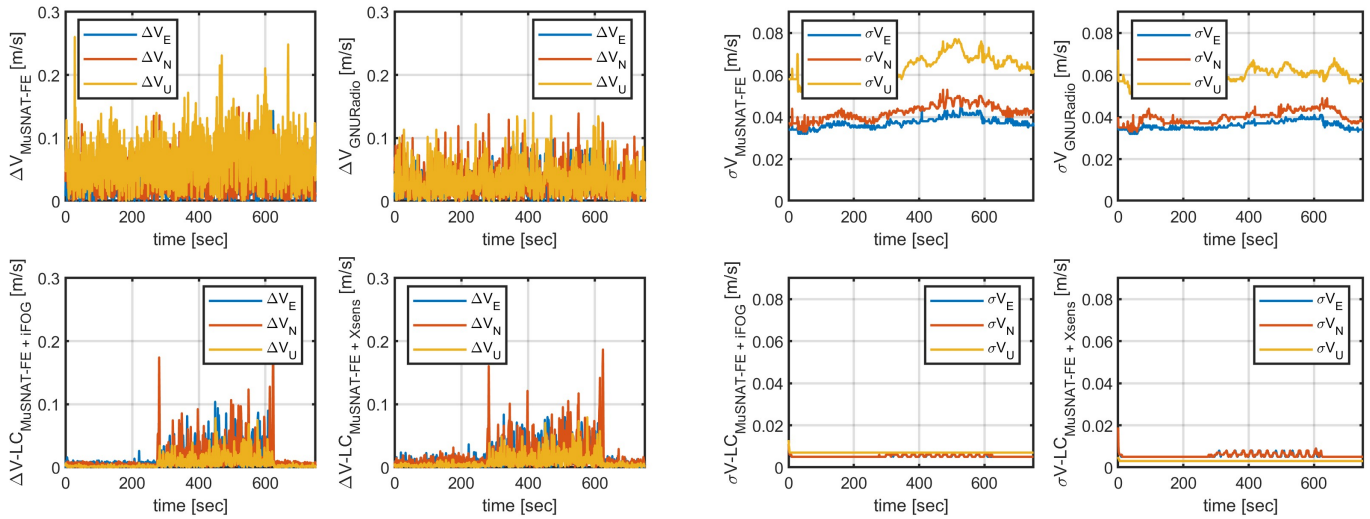

Figure 10: Deviation of the estimated velocity w.r.t. the ground-truth trajectory (left sub-plots) in east, north and upward direction. Right figures show the velocity standard deviation as estimated by TerraPos.

absolute position (see Figure 9, right plots) reveals that both positioning results need similar convergence time (2-4 seconds) to achieve stable precision of about 1-2 cm.

Giving the fact that in a LC fusion strategy the position information have to be computed beforehand and later fused with the IMU signal in common filter, usually EKF, the accuracy of the GNSS observation will dictate the accuracy of the fusion outcome. Therefore, in open-sky conditions, the inertial sensor will be mostly in charge of interpolating the trajectory to higher sampling rates and also providing attitude information. In this case, the benefit of augmenting the positioning engine with IMU-observation will be, barely, visible, which is the case in our experiment. Nevertheless, the successful processing of their raw data by means of the TerraPos-software will indicates successful realisation of these sensors. i.e iFOG- and Xsens-IMUs, with our MuSNAT-FE. This performance has been already achieved, which can be validated by the lower plots in Figure 9, i.e. ΔP-LC$_{\text{MuSNAT-FE + iFOG}}$ and ΔP-LC$_{\text{MuSNAT-FE + Xsens}}$. In details, in case of using the iFOG-IMU the deviation from the reference trajectory in comparison remains almost identical, however, this difference increases with the low-cost Xsens-IMU, where a maximum error of 6.7 cm and RMS of 3.3 cm can been seen in the north direction. The main reason for this degradation, especially, for for the Xsens, can be explained by the lack of high accurate senor calibration (only manufacturer specification have been used here) and the unknown

internal hardware timing bias, i.e., the elapsing time after the trigger plus generated by the MuSNAT-FE (see Fig.1), is received to send the IMU data packages. On the other side, the hardware timing bias of iFOG-IMU, is well known as it is provided by the manufacturer, so that a high-accurate and reliable time stamping of the iIMU-signals is possible. Such error source can make tuning of the EKF, c.g., in TerraPos, very cumbersome and therefore difficult to improve the accuracy of the navigation, especially, in case of the blockage of the satellites signals. The same behaviour and performance can observed in both velocity deviation and its standard deviation of these different fusing strategies (see Figure 10). The appropriate statistics are summarized in Table 2.

Table 1: Estimated RMS values using the GNSS/INS-TerraPos software

Processing combination	E [m]			N [m]			U [m]		
	Max	Min	RMS	Max	Min	RMS	Max	Min	RMS
$\Delta P_{\text{MuSNAT-FE}}$	0.017	0.003	0.009	0.013	0.003	0.004	0.033	0.001	0.018
$\Delta P_{\text{GNURadio}}$	0.007	0.002	0.002	0.010	0.002	0.002	0.012	0.002	0.004
ΔP-LC$_{\text{MuSNAT-FE + iFOG}}$	0.019	0.001	0.010	0.023	0.002	0.009	0.026	0.001	0.014
ΔP-LC$_{\text{MuSNAT-FE + Xsens}}$	0.037	0.002	0.014	0.067	0.001	0.032	0.034	0.002	0.013

Table 2: Estimated RMS values using the GNSS/INS-TerraPos software

Processing combination	V_E [m/s]			V_N [m]			V_U [m/s]		
	Max	Min	RMS	Max	Min	RMS	Max	Min	RMS
$\Delta V_{\text{MuSNAT-FE}}$	0.14	0.01	0.03	0.15	0.01	0.04	0.26	0.01	0.08
$\Delta V_{\text{GNURadio}}$	0.12	0.02	0.03	0.14	0.00	0.04	0.14	0.02	0.04
ΔV-LC$_{\text{MuSNAT-FE + iFOG}}$	0.12	0.01	0.02	0.20	0.01	0.03	0.08	0.01	0.01
ΔV-LC$_{\text{MuSNAT-FE + Xsens}}$	0.08	0.02	0.02	0.19	0.02	0.03	0.08	0.03	0.01

Table 3: Estimated IMU timing bias using the GNSS/INS-TerraPos software

	bias [ms]	precision [ms]	accuracy [ms]
LC MuSNAT-FE + iFOG IMU	0.85	1.98	< 0.001
LC MuSNAT-FE + Xsens IMU	7.64	2.70	< 0.001

Table 3 summarises the estimated timing bias of both used IMUs. The estimated bias for the iFOG is below 1 ms while the same bias for the Xsens is approx. 7 times higher. The accuracy of both biases are below 1 microseconds. That means, the bias can be estimated very accurately and it remains constant over time, which can be compensated within any fusion software as a calibration parameter.

VII. USRP FREQUENCY SYNTHESIS: FRAC-N VERSUS INT-N MODE

During our measurement campaign, we observed significant phase residuals in the carrier-phase data of the MuSNAT-FE, leading to 57.5% float relative position solutions. As mentioned in previous sections, this phenomenon is likely attributed to the implementation of the PLL in the front end. The PLL is responsible for aligning the phase and frequency of the generated (output) signal with a reference signal, employing either fractional (frac-n) or integer (int-n) mode. Depending on the selected mode, the PLL reference frequency results from the division of the front-end daughterboard clock frequency by an integer or fractional divider, respectively. The default mode for the PLL in the MuSNAT-FE is fractional (frac-n), which introduces spurious tones and fails to perfectly align the intermediate frequency (IF) signal at the desired center frequency. This erroneous effect is visible in the in-phase and quadrature (IQ) samples collected with the MuSNAT-FE. To validate our assumption that the frac-n mode PLL implementation affects the real-time kinematic (RTK) positioning results, we developed and deployed a second front-end system. This second system comprises a USRP X310 front end and a GNU Radio companion (GNC) (GNU Radio project, 2022) recording flowchart, which tunes the PLL mode in int-n or frac-n mode. For simplicity, we will refer to the MuSNAT frac-n and the USRP X310 int-n implementations as MTfrac and X310int, respectively. Before deploying the MTfrac and X310int in the van test, we conducted multiple successive long static recording campaigns with the X310int linked to a 10 MHz external clock in frac-n and int-n mode, ingesting a sine wave signal with a central frequency of 1.570001 GHz sampled at 200 kHz. The upper section of Figure 11 provides a detailed comparison of the magnitude and phase characteristics of IQ samples obtained during a static test using the X310int in frac-n and int-n modes. Notably, the magnitude of IQ samples from the frac-n implementation (in blue in the lower part of Figure 11) exhibits oscillations, in contrast to the smoother int-n magnitude (in green in the lower part of Figure 11). The int-n magnitude displays a spread approximately 37% smaller than that of the frac-n implementation. Furthermore, the frac-n implementation introduces a slight increase in phase noise (in red as opposed to yellow), as observed in the upper section of Figure 11. The combination of oscillating magnitude and increased phase noise in the IQ samples from the frac-n PLL likely contributes to significant carrier-phase errors, thereby impacting the accuracy of RTK positioning.

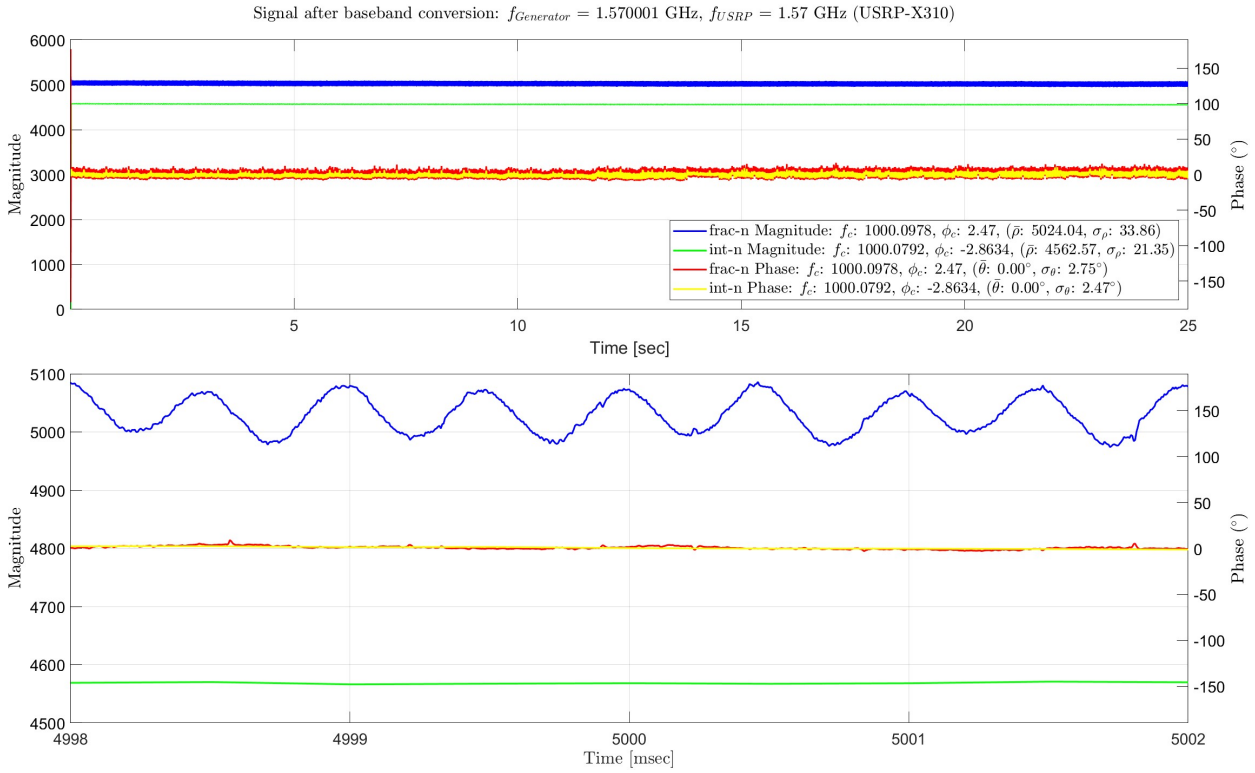

Figure 11: Comparison of magnitude and phase (top) of a short IQ data recorded in frac-n (blue for magnitude and red for phase) and int-n (green for magnitude and yellow for phase) modes with X310int. The lower section of the figure provides a zoomed-in preview of the magnitude and phase information. Notably, the magnitude of IQ samples from the frac-n implementation (blue) shows oscillations contrasting with the smoother int-n magnitude (green), which has a spread of 37% smaller. Additionally, the frac-n implementation introduces a slight increase in phase noise (red vs yellow), observable in the top portion of the figure.

Returning to the van campaign described in Section VI, when examining combined (forward + backward) RTK GPS L1 + Galileo L5 position results using kinematic code and carrier-phase data, we observed a position fixing rate of 42% and 100% with the MTfrac and X310int implementations, respectively. Based on these results, it becomes evident that an int-n PLL implementation is more favorable for achieving improved RTK positioning outcomes. We believe that an int-n PLL implementation favors better RTK positioning results, opening up a interesting research subject for further exploration. But it also noted, that by applying a frequency offset while using the frac-n mode, the ambiguity fixing rate can be increased to 100% as described above. Thus for most of our navigation research the frac-n mode will work fine, but for utmost precision, the int-n mode might be preferable.

VIII. CONCLUSION

This paper introduced the front-end development of the Institute of Space Technology and Applications of the University of the Bundeswehr Munich, which is based on the USRP-2955 of NI. It provides four radio-frequency channels with inertial measurement unit support. We demonstrated that it can achieve PPP solutions with an accuracy of three centimeter. New functions are added, which includes an automatic gain control and a decimation of the bit resolution of the radio-frequency data, the interface for the IMUs to enable a synchronized IMU recording, and a calibration of the frequency accuracy. It was shown that the USRP does have a very small systematic error of the absolute frequency for some frequency bands, which needs to be compensated for obtaining a PPP solution. This offset to the center frequency was determined empirically. Future work shall provide a more precise determination of the frequencies. Two proposals are discussed within this paper. Further work includes establishing of TCP/IP based streaming of GNSS and IMU data, direct use of the IMU time stamps during GNSS/INS integration and support of the ION SDR Standard.

ACKNOWLEDGEMENTS

The results presented in this work were developed within the projects “SeRANIS – Seamless Radio Access Networks for Internet of Space” funded by the dtec.bw – Digitalization and Technology Research Center of the Federal Armed Forces of Germany under Grant 150009910 and “Forschungs- und Studienvorhaben für Innovationen des Galileo GNSS-Systems (GalileoFUSION-II)”

funded by the German Federal Ministry for Economic Affairs and Climate Action (BMWK) and administered by the Project Management Agency for Aeronautics Research of the German Space Agency (DLR) in Bonn, Germany (grant no. 50NA2301).

We would like to thank Jade Morton and Steve Taylor from the University of Colorado Boulder for their support on the topic of USRPs and their frequency accuracy.

REFERENCES

Arizabaleta, M., Ernest, H., Dampf, J., Kraus, T., Sanchez-Morales, D., Dötterböck, D., Schütz, A., and Pany, T. (2021). Recent Enhancements of the Multi-Sensor Navigation Analysis Tool (MuSNAT). In *Proceedings of the 34th International Technical Meeting of the Satellite Division of The Institute of Navigation (ION GNSS+ 2021)*, ION GNSS+, The International Technical Meeting of the Satellite Division of The Institute of Navigation, pages 2733–2753. Institute of Navigation.

GNU Radio project (2022). GNU Radio, version 3.10.1.

Kjørsvik, N. S. and Brøste, E. (2009). Using TerraPOS for efficient and accurate marine positioning. *TerraTec AS, Lysaker, Norway, White paper*.

Lotz, T. (2008). *Adaptive Analog-to-Digital Conversion and pre-correlation Interference Mitigation Techniques in a GNSS receiver*. Diploma Thesis, Technische Universität Kaiserslautern.

Pany, T., Dötterböck, D., Gomez-Martinez, H., Hammed, M. S., Hörkner, F., Kraus, T., Maier, D., Sanchez-Morales, D., Schütz, A., Klima, P., and Ebert, D. (2019). The Multi-Sensor Navigation Analysis Tool (MuSNAT) – Architecture, LiDAR, GPU/CPU GNSS Signal Processing. In *Proceedings of the 32nd International Technical Meeting of the Satellite Division of The Institute of Navigation (ION GNSS+ 2019)*, ION GNSS+, The International Technical Meeting of the Satellite Division of The Institute of Navigation, pages 4087–4115. Institute of Navigation.

Titterton, D. and Weston, J. (2005). *Strapdown Inertial Navigation Technology, Second Edition (Progress in Astronautics and Aeronautics)*. AIAA.